

Photoluminescence and Raman studies of GaN films grown by MOCVD

This content has been downloaded from IOPscience. Please scroll down to see the full text.

2009 J. Phys.: Conf. Ser. 187 012021

(<http://iopscience.iop.org/1742-6596/187/1/012021>)

View [the table of contents for this issue](#), or go to the [journal homepage](#) for more

Download details:

IP Address: 140.113.38.11

This content was downloaded on 25/04/2014 at 13:08

Please note that [terms and conditions apply](#).

Photoluminescence and Raman studies of GaN films grown by MOCVD

Luong Tien Tung^{1,3}, K L Lin¹, E Y Chang¹, W C Huang¹, Y L Hsiao¹ and C H Chiang²

¹ CSD Lab, Department of Materials Science and Engineering, National Chiao Tung University, Taiwan R. O. C.

² Department of Electrophysics, National Chiao Tung University, Taiwan R.O.C.

³ Faculty of Physics, Hanoi National University of Education, Vietnam

E-mail: tungluongtien@gmail.com

Abstract. The photoluminescence (PL) of high quality GaN epitaxial layer grown by MOCVD was investigated for various excitation power and temperatures from 8.3 to 300K. The PL at 8.3 K and with relatively low excitation power of GaN film grown on c-plane sapphire by using MOCVD shows clearly free-exciton A, B and exciton A bound to neutral donors (D^0X) at 3.502 eV, 3.509 eV, and 3.496 eV, respectively. The full width at half maximum (FWHM) and binding energy of exciton A of the high quality GaN film were evaluated as small as 3.7 meV and 27.9 ± 0.5 meV, respectively. In addition, PL and Raman scattering of GaN films grown on r-plane sapphire and (111) Si substrates by using MOCVD were examined. The residual stress effect was detected in all films.

Keyword: Metalorganic chemical vapour deposition, GaN, photoluminescence, binding energy, Raman.

1. Introduction

Gallium nitride (GaN) and its alloys with InN and AlN have emerged as important semiconductor materials with applications to green, blue, and ultraviolet portions of the spectrum as emitters and detectors and to high-power/temperature radio frequency electronic devices. GaN is probably the most important semiconductor since silicon due to their direct and wide band gap, high saturation velocity and high breakdown field. Metal-organic chemical vapour deposition (MOCVD) is currently the most widely used technology. Usually, all optoelectronic commercial device structures are fabricated using MOCVD. Recently, the high quality GaN grown on sapphire or on low cost Silicon substrate by MOCVD have been investigated with low density of threading dislocations (TDs) suitable for Blue LEDs and UV LEDs, which require dislocation densities lower than 10^8 cm⁻² [1]. Photoluminescence (PL) and Raman are the most powerful methods to study material. The quality of GaN material relates to pure free exciton transition. However, some experimental data appear conflicting, an example of very low value for binding energy of free exciton A (FX_A) in GaN layer grown on sapphire substrate [2 - 4], which is expected to be larger than 27 meV in unstrained GaN. It could be due to the incorrect labelling of free exciton peaks or a mistake of temperature range of pure exciton transition.

In this paper, photoluminescence (PL) and Raman spectra of GaN grown on sapphire and silicon substrate by MOCVD have been examined. The re-combination mechanism in different ranges of

temperature was clearly made and the residual strain in GaN layers was deduced from detailed analysis of the energy shift observed on the Raman spectra.

2. Experimental

The 1- μm thick GaN layers were grown at 1080°C by MOCVD on c-plane, r-plane sapphire and (111) oriented Silicon substrates with different buffer layers, low temperature GaN buffer layers, high-low-high temperature (H-L-H Temp.) GaN or AlN layers for instance. The PL measurements were carried out using a Spectra Pro PL system with a He–Cd laser operating at 325 nm as an excitation source. Temperature was controlled between ~ 8 K and 325 K using a closed-cycle cryostat. All the Raman spectra have been recorded with a double grating spectrometer in backscattering geometry, at room temperature; the He–Ne laser (632.8 nm) was used for the excitation. The diameter of the spot in the sample was typically 1 μm .

3. Results and discussion

Figure 1 presents PL spectra of GaN on c-plane sapphire measured at 14 K. The PL spectra exhibits the dominant transition of near band-edge (NBE) band at 3.5013 eV, together with shoulder at higher energy of 3.509 eV and another at lower energy of 3.496 eV. The inset exhibits three emission lines identifying as the shallow neutral donor-bound (D^0X) and free exciton (FX_A and FX_B), the bound-exciton (D^0X) level exist 5.7 meV below the free exciton (FX_A) energy. The splitting of FX_A and FX_B levels is 6.6 meV. Our results agree with [5, 8], and the linewidths of D^0X , FX_A and FX_B as small as 4.0, 3.9 and 6.9 meV, respectively, show the high quality crystal of GaN layer [5, 6, 7]

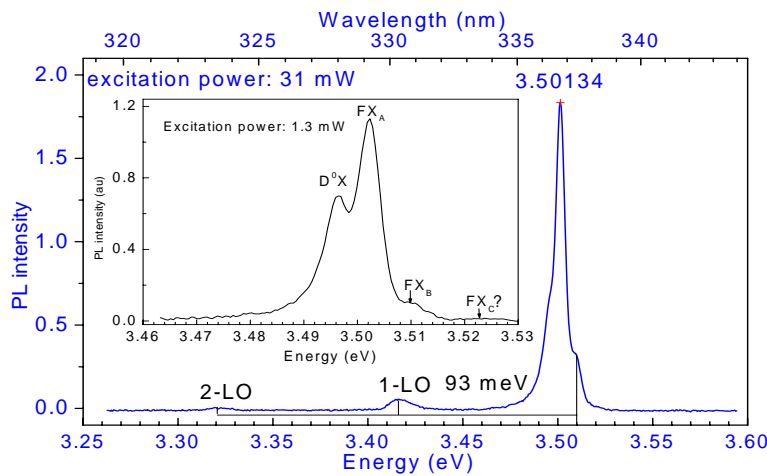


Figure 1. (a) PL spectra of GaN on sapphire at 14 K and 31 mW of excitation power. Inset: near band-edge band of GaN at 14 K and 1.3 mW excitation power.

The temperature dependence of GaN film was investigated. The redshift and broadening of all emission lines with increasing temperature were observed. The temperature dependence of the linewidth is attributed to phonon-induced band broadening [9]. The characteristic redshift with increasing temperature is attributed to band gap reduction from lattice expansion and to electron-phonon interactions [10]. The first contribution has major play at low temperature. In figure 2a, the temperature dependence of the energy position of lines (D^0X , FX_A , and FX_B), therefore, is similar and the energy level difference between at 14 K and at 85 K is 4.9 meV. As the temperature increases, the quick decrease in PL intensity was observed and the shallow neutral donor-bound (D^0X) transition is extinguished above 100 K. In figure 3b, we show PL intensity variation as a function of temperature and the fit curves were described by formula:

$$I(T) = \frac{I(0)}{1 + C_1 \exp\left(-\frac{\Delta E_1}{kT}\right) + C_2 \exp\left(-\frac{\Delta E_2}{kT}\right)}, \quad (3)$$

where, ΔE is activation energy. The thermal quenching of the FX_A exciton is satisfactorily fitted with

two nonradiative processes with activation energies of 5.7 ± 0.5 meV and 27.9 ± 0.5 meV, respectively. The first process is attributed to the change of the exciton from the lower branch of the *A* exciton to the branch of the *B* exciton [11]. The increase of the population in the *B* branch is also evidenced by the enhancement of FX_B intensity in the temperature range lower 25 K (figure 3b). At higher temperature (> 40 K) the PL intensity of FX_A and FX_B quench with the same activation energy (27.9 meV), it has been reported that the binding energy of the *A* and *B* exciton are almost the same and the excitons binding energy of GaN/c-plane sapphire are slightly larger than in unstrained GaN ($\sim 26 - 27$ meV) [11-15].

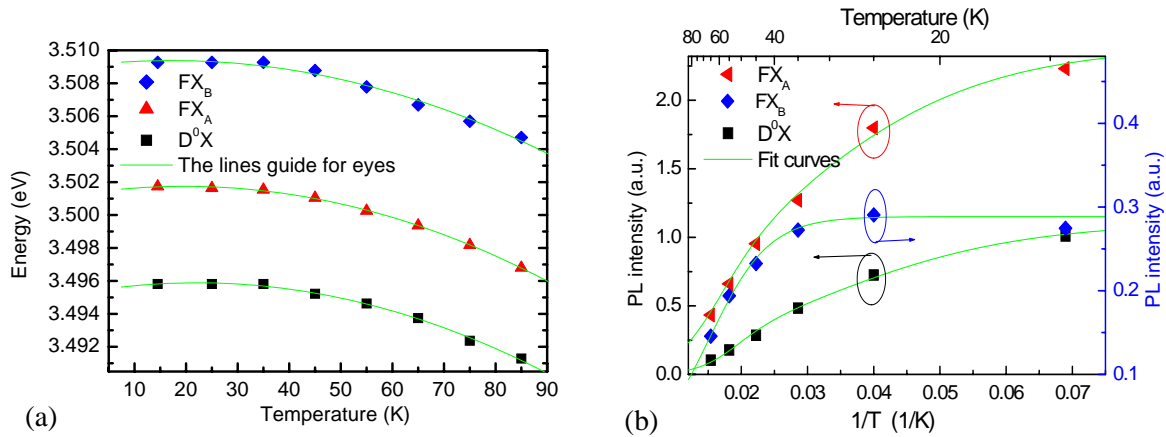


Figure 3. The temperature dependence of energy position of GaN/sapphire (a) and PL intensity various $1/T$; (b) of FX_B (◆-diamond), FX_A (▲-triangle), and D^0X (■-square). The fit curves were described by formula (1).

The quenching of the donor-bound exciton D^0X emission is also described by two nonradiative processes. The first process is assigned for thermal destruction of shallow donor–exciton bound with activation energy of 5.3 ± 0.5 meV. This value is in a good agreement with the difference of energy level between D^0X and FX_A . The second process with activation energy of 32.3 ± 0.5 meV can be attributed to the ionization of the donors or to a simultaneous exciton delocalization and exciton dissociation [11, 16]. This value is in excellent agreement with the binding energies of Si_{Ga} and O_N donors, 30.18 ± 0.1 and 33.2 ± 0.1 meV, respectively [17].

At low temperatures and low excitation densities, free carriers can form free exciton states or become bound to impurities so that the luminescence spectra are dominated by these states rather than by band-to-band recombination. However, the band-to-band transition cannot be ignored at higher temperature. The excitation power-dependent photoluminescence has been widely used for determining the origin of light emission in semiconductors, $I_{PL} = \mu I_{laser}^\alpha$ (2) [18, 19]. In this relation, it is predicted that for free-exciton recombination $\alpha \approx 1$; for band gap recombination, i.e., free-carrier electron-hole bimolecular recombination, $\alpha \approx 2$; and for the intermediate case involving free exciton and free carriers $1 < \alpha < 2$. Table 1 shows the α values and recombination mechanism of transitions in different ranges of temperature.

Table 1. The α values in different ranges of temperature. The coefficient α is obtained by fitting the measured power dependence of the luminescence lines by $I_{PL} = \mu I_{laser}^\alpha$ formula.

	D^0X	FX_A	NBE	NBE
Temp. range	8.3 K	8.3 – 75 K	100 – 300 K	375 – 450 K
α	$\sim 1^a$	~ 1	1.5 – 1.73	~ 2
Recombination mechanism	Donor bond exciton	Pure free exciton	Both free exciton and free carriers band-to-band	Free carriers band-to-band

^a This value is obtained at low range of excitation power (< 5 mW).

In addition, the dependence of PL intensity of D⁰X on excitation power at 8.3 K is shown in figure 4a. It saturates at about 12 mW. The decrease of PL intensity and the redshift of energy of FX_A as the excitation power increases higher than 15 mW because of the inelastic exciton-exciton interaction are presented in figure 4a and 4b. It implies that the accuracy of calculating values must be based on the measurements at sufficiently low excitation power and low range temperature (3.6 mW and lower 85 K in our experiments).

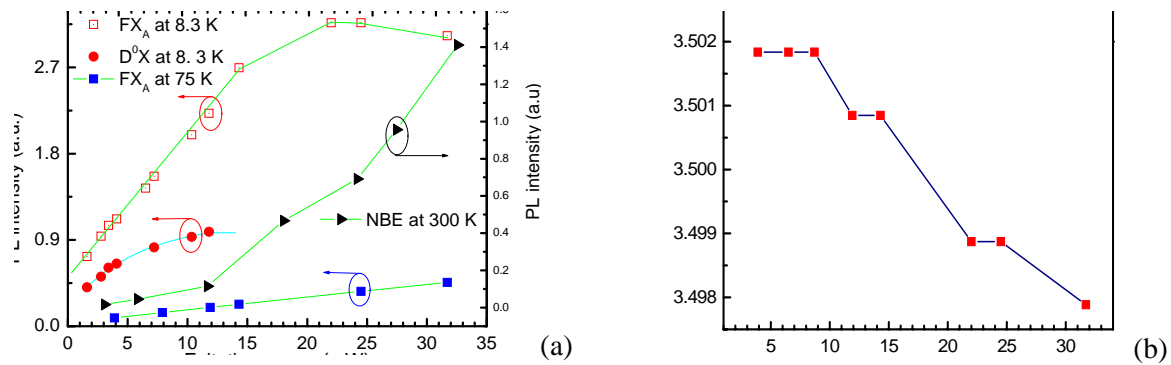


Figure 4. (a) The PL relative intensity of GaN/sapphire: FX_A at 8.3 K (□ open square), D⁰X at 8.3 K (● circle), FX_A at 75 K (■ solid square), and near band-edge emission (NBE) (▶ triangle) and (b) energy of FX_A at 8.3 K at various excitation power.

Growth of GaN on r-plane sapphire substrate is expected to improve the efficiency of light emitting diodes (LEDs) by removing the spontaneous polarization and the piezoelectric fields to the quantum wells active layer based on heterostructure [21-24]. In contrast with GaN/c-plane sapphire substrate, the GaN/r-plane sapphire has significantly higher density of the basal plane (0001) stacking faults (BSFs) because of the planar anisotropic nature of the growing surface [25]. The BSFs play role as luminescence active centers in GaN layer.

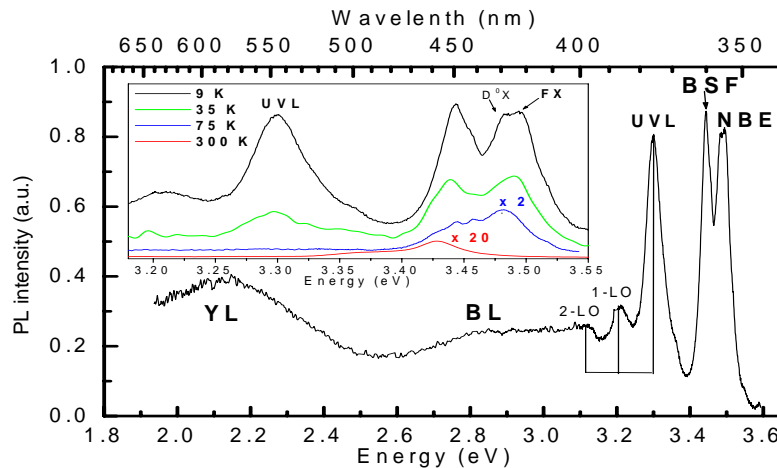


Figure 5. Typical PL spectra of GaN/r-plane sapphire substrate grown by MOCVD measured at 9K. Inset: PL spectra at different temperatures. Note PL intensity is magnified by 2 at 75 K and by 20 at 300 K.

Figure 5 shows the typically PL spectra of GaN grown on r-plane sapphire by MOCVD measured at 9 K. NBE emission band involving free exciton FX transition energy of 3.494 eV and D⁰X transition energy of 3.484 eV was observed. The band labelled BSF at 3.443 eV belongs to basal plane stacking faults [26, 27]. It is a specific band in GaN on non-c-plane sapphire substrate and dominant at low temperature. In examining GaN/c-plane sapphire, the broad band at 3.300 eV which followed by LO replica sidebands separated by 91 meV contributes to both donor-acceptor-pair (DAP) and free-electron-acceptor (e-A) emission, called ultra-violet luminescence band (UVL) [14]. In particular, in GaN/r-plane sapphire, UVL also is contributed by the transitions related to prismatic stacking faults

formed on $\{11\bar{2}0\}$ planes [26, 28, 29]. In inset of figure 5, PL spectra at different temperature reveal very fast thermal quenching of UVL band due to primarily related ionization of acceptors and donors by heating. While BSFs act as the quantum-well-like region confine electrons. Thus, BSFs emission can be observed at elevated temperatures [26]. Two very broad bands, a blue band (BL) at about 2.85 eV and a yellow band (YL) at about 2.1 meV, have been detected. In undoped GaN, the BL band is caused by transition from shallow donors (at low temperature) or conduction band to relatively deep acceptor (Zn_{Ga}), from Zn contamination by impure gases used in MOCVD, while the YL band relates to V_{Ga} or V_{Ga} -complex, such as $V_{Ga}O_N$ or $V_{Ga}Si_N$ [14]. Although the spontaneous polarization and the piezoelectric fields can be eliminated from AlGaN/GaN heterostructure, the high density of basal plane stacking faults (BSFs) is a big challenge in growth GaN on r-plane sapphire substrate by MOCVD, so far.

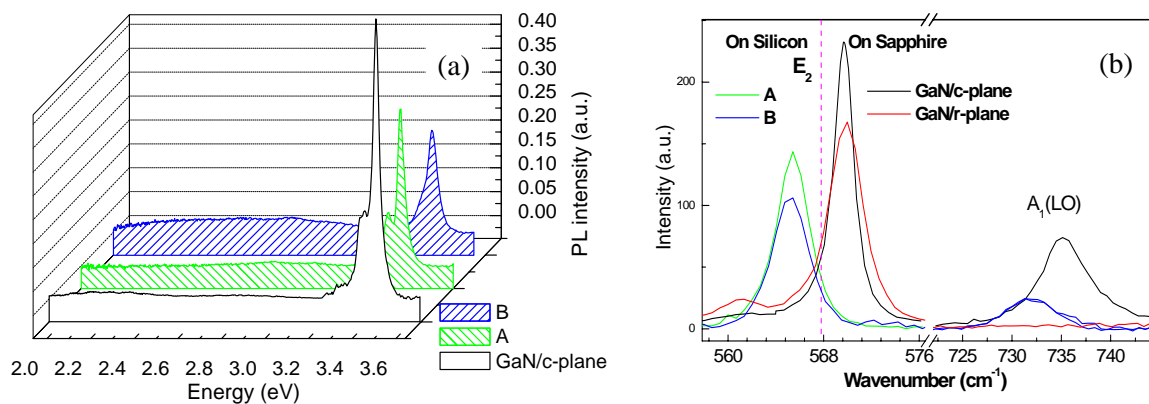


Figure 6. (a) Room temperature PL spectra of GaN grown on c-plane sapphire and on silicon substrates; (b) Raman spectra of GaN grown on silicon substrates (A, B); on c-plane, c-plane sapphire substrate at room temperature. The vertical dotted line denotes E_2 mode frequency position of strain-free GaN of 567.6 cm^{-1} at room temperature.

GaN grown on silicon substrate lowers cost and uses better heat dissipation in comparison with sapphire substrates but it is not as good as GaN grown on sapphire substrate. In figure 6a, we show room temperature PL of two samples, called A and B grown on silicon substrates using the same buffer layer structure H-L-H temperature AlN; and GaN grown on c-plane sapphire substrate. The PL spectra reveal that both samples A and B have the NBE band at the same energy position of 3.40 eV dominantly attributed to band-to-band transition. The NBE band is more broadened, however, and the blue band (BL) and yellow band (YL) relate to the defects are clearly observed in the B sample. It is indicated that there is higher defects dislocation in the B sample than in the A sample. In the GaN grown on c-plane sapphire substrate, the NBE band at 3.43 eV is very strong and sharp, while YL band cannot hardly be nearly observed. The NBE band shift can be caused not only by strain but also strongly by the Burstein-Moss effect. Therefore, we move to study Raman measurement of the E_2 Raman mode that is known to be shifted by stress only [30]

Raman is a powerful method to examine quality and to monitor residual stress of the GaN film. The width of the strongest mode E_2 (high) can be used to analyze lattice defects [5, 31], whereas its frequency shift can be well used to monitor residual stress [5, 32, 33]. The residual stress due to mismatch of the lattice constants and the thermal expansion coefficients of the substrate and epitaxial film significantly effects the optical and electrical properties of epitaxial film. The differences in thermal expansion coefficients between layers and substrates dominantly contribute to the residual strain [31]. Usually, growth GaN films on sapphire substrates induce compressive strains and on silicon substrates induce tensile strains. The E_2 mode of strain-free GaN is known to be 567.6 cm^{-1} at room temperature [31, 34].

In investigating, Raman spectra of all samples were measured at room temperature. The measured Raman spectra of all samples are presented in figure 6b. The upshift of the E_2 peak frequencies is corresponding to compressive strain, GaN grown on sapphire substrates, whereas the tensile strain in GaN grown on silicon substrates is observed by the decrease in E_2 mode frequency in comparison to strain-free GaN. While E_2 mode is only affected by residual stress and crystalline quality. The $A_1(\text{LO})$ mode depends not only on the residual stress in GaN film but also on the coupling to free carriers (plasmon) of LO mode [35, 36]. It is beyond the scope of study in this work. The frequencies position and linewidth of E_2 peaks at room temperature of all samples given in table 1. The Raman shift and linewidth (Γ , full width at half maximum) are determined by fitting Lorentzian functions to the experimental data.

Table 2. Energy position, linewidth of NBE bands, frequencies position and linewidth of E_2 peaks at room temperature of all samples.

Sample	E_2 (cm^{-1})	Γ of E_2 (cm^{-1})
GaN/c-plane sapphire	569.68	1.98
GaN/r-plane sapphire	569.86	3.25
A (GaN/silicon)	565.40	3.40
B (GaN/silicon)	565.22	3.70
References	567.6 [31,34]	1.75 [5]; 2.0 [31]

Linewidth of B sample is larger than that of A sample to indicate that B sample has higher defects density than A sample, this result is good in agreement with above PL examination. The linewidth of E_2 peak is as narrow as 1.98 cm^{-1} compares well with previously published reports [5, 7, 31] indicating very low defects density in GaN grown on c-plane sapphire sample. In comparison to A and B samples, the influence of defects on the shift of E_2 peak is small. Thus, we can neglect the hydrostatic stress component, which can arise from point defects in low quality GaN or even from dopants in doped GaN layers. For pure biaxial stress, the frequency shift of the E_2 phonon with respect to unstrained GaN is related to stress-induced changes the E_2 phonon Γ of $4.2 \text{ cm}^{-1} \text{ GPa}^{-1}$ [37]. The upshifted E_2 frequency in GaN film grown on c-plane sapphire corresponds to a compressive stress of 0.5 GPa and higher values in the other samples.

4. Conclusion

GaN films grown by MOCVD on different substrates were examined by Photoluminescence (PL) and Raman measurement. We show that in the high quality crystal GaN grown on c-plane sapphire, the PL linewidth of free exciton A transition at 8.3 K and Raman E_2 mode line are as small as 3.7 meV and 1.98 cm^{-1} , respectively. Thermal quenching of the different transitions was observed by study dependent temperature PL. It reveals very fast thermal quenching of the transitions relating to exciton bond to acceptors, donors, or dislocations. The binding energy of free exciton A and B in compressive strain GaN/c-plane sapphire are the same of 27.9 meV and slightly higher than that in strain-free GaN. The pure free exciton recombination is just at a very low temperature. We also point out that for accuracy of above calculations the measurements necessarily have to carry out at sufficiently low range of temperatures and excitation power. In comparison with GaN/c-plane, the GaN films grown on r-plane and silicon substrates are higher residual stress and lower quality crystal.

References

- [1] Gibart P 2004 *Pep. Prog. Phys.* **67** 667-715
- [2] Smith M, Chen G D, Lin J Y, Jiang H X, Asif-Khan M, Sun C J, Chen Q, Yang J W 1996 *J. Appl. Phys.* **79**, 7001-7004
- [3] Smith M, Chen G D, Li J Z, Lin J Y, Jiang H X, Salvador A, Kim W K, Aktas O, Morkoc A 1995 *Appl. Phys. Lett.* **67**, 3387-3389

- [4] Reynolds D C, Look D C, Kim W, Aktas O, Botchkarev A, Salvador A, Morkoc H 1996 *Appl. Phys.* **80**, 594-596
- [5] Song D Y, Basavaraj M, Nikishin S A, Holtz M, Soukhoveev V, Usikov A and Dmitriev V 2006 *J. Appl. Phys.* **100** 113504
- [6] Keller S, Keller B P, Wu Y-F, Heying B, Kapolnek D, Speck J S, Mishra U K and DenBaars S P 1996 *Appl. Phys. Lett.* **68** (11) 1525
- [7] Martínez O, Avella M, Jimenez J, Gerard B, Cusco R and Artus L 2004 *J. Appl. Phys.* **96** 3639
- [8] Shan W, Schmidt T J, Yang X H, Hwang S J, Song J J and Goldenberg B 1995 *Appl. Phys. Lett.* **66** 985
- [9] Rudin S, Reinecke T L and Segall B 1990 *Phys. Rev. B* **42** 11218
- [10] Capaz R B, Spataru C D, Tangney P, Cohen M L and Louie S G 2005 *Phys. Rev. Lett.* **94** 036801
- [11] Paskov P P, Paskova T, Holtz P O and Monemar B 2004 *Phys. Rev. B* **70** 035210
- [12] Monemar B, Bergman J P, Buyanova I A, Li W, Amano H and Akasaki I 1996 *Material Research Soc. Internet Journal of Nitride Semiconductor Research* **1** 2
- [13] Eckey L, Holst J.-Chr, Hoffmann A, Broser I, Detchprohm T and Hiramatsu K 1997 *Material Research Soc. Internet Journal of Nitride Semiconductor Research* **2** 1
- [14] Reshchikov M A and Morkoç H 2005 *J. Appl. Phys.* **97** 061301
- [15] Rodina A V, Dietrich M, Göldner A, Eckey L, Hoffmann A, Efros Al L, Rosen M and Meyer B K 2001 *Phys. Rev. B* **64** 115204
- [16] Leroux M, Grandjean N, Beaumont B, Nataf G, J Massies and Gibart P 1999 *J. Appl. Phys.* **86** 3721
- [17] Moore W J, Freitas J A, Lee S K, Park S S and Han J Y 2002 *Phys. Rev. B* **65** 081201
- [18] Fouquet J E and Siegman A E 1985 *Appl. Phys. Lett.* **46** 280
- [19] Bergman L, Cheng X B, Morrison J L and Huso J 2004 *J. Appl. Phys.* **96** 675
- [20] Chen X B, Huso J, Morrison J L and Bergman L 2006 *J. Appl. Phys.* **99** 046105
- [21] Bernardini F, Fiorentini V and Vanderbilt D 1997 *Phys. Rev. B* **56** R10024
- [22] Lefebvre P *et al.* 2001 *Appl. Phys. Lett.* **78** 1252
- [23] Nishida T and Kobayashi N 1999 *Phys. Stat. Sol. (a)* **176** 45
- [24] Fiorentini V, Bernardini F, Sala F.D, Carlo A D and Lugli P 1999 *Phys. Rev. B* **60** 8849
- [25] Paskov P P, Paskova T, Holtz P O and Monemar B 2001 *Phys. Rev. B* **64** 115201
- [26] Paskov P P, Schifano R, Monemar B, Paskova T, Figge S and Hommel D 2005 *J. Appl. Phys.* **98** 093519
- [27] Wu Z H, Fischer A M, Ponce F A, Bastek B, Christen J, Wernicke T, Weyers M and Kneissl M 2008 *Appl. Phys. Lett.* **92** 171904
- [28] Liu R, Bell A, Ponce F A, Chen C Q, Yang J W and M Khan A 2005 *Appl. Phys. Lett.* **86**, 021908
- [29] J Mei, S Srinivasan, Liu R, Ponce F A, Narukawa Y and Mukai T 2006 *Appl. Phys. Lett.* **88** 141912
- [30] Perlin P, Jauberthie-Carillon C, Itie J P, Miguel A S, Grzegory I and Polian A 1992 *Phys. Rev. B* **45** 83
- [31] Kitamura T, Nakashima S, Nakamura N, Furuta K and Okumura H 2008 *Phys. Stat. Sol. (c)* **5** No. 6 1789
- [32] Inoue T, Toda Y, K Hoshino, Someya T and Arakawa Y 2003 *Phys. Stat. Sol. (c)* **0** No. 7 2428
- [33] Park H J, Park C, Yeo S, Kang S.W, Mastro M, Kryliouk O, and Anderson T J *Phys. Stat. Sol. (c)* **2**, No. 7, 2446 (2005).
- [34] Davydov V Yu, Kitaev Yu E, Goncharuk I N, Smirnov A N, Graul J, Semchinova O, Uffmann D, Smirnov M. B, Mirgorodsky A. P. and Evarestov R. A. 1998 *Phys. Rev. B* **58** 12899
- [35] Kozawa T, Kachi T, Kano H, Taga Y, and Hashimoto M, Koide N and Manabe K 1994 *J. Appl. Phys.* **75** (2) 1098
- [36] Kuball M 2001 *Surf. Interface Anal.* **31** 987–999

- [37] Kisielowski C, Kruger J, Ruvimov S, Suski T, Ager J W III, Jones E, Liliental-Weber Z, Rubin M, Weber E R, Bremser M D and Davis R F 1996 *Phys. Rev. B* **54** 17745

Acknowledgments

This work was supported by the Ministry of Economic Affairs and the National Science Council of the Taiwan under the contracts: NSC 96-2752-E-009-001-PAE and 96-EC-17-A-05-S1-020.